Chapter 15

Waves

15.1 Overview

In the preceding chapters, we have derived the basic equations of fluid dynamics and developed a variety of techniques to describe stationary flows. We have also demonstrated how, even if there exists a rigorous, stationary solution of these equations for a time-steady flow, instabilities may develop and the amplitude of oscillatory disturbances can grow with time. These unstable modes of an unstable flow can usually be thought of as waves that interact strongly with the flow and extract energy from it. Waves, though, are quite general and can be studied quite independently of their sources. Fluid dynamical waves come in a wide variety of forms. They can be driven by a combination of gravitational, pressure, rotational and surface-tension stresses and also by mechanical disturbances, such as water rushing past a boat or air passing through a larynx. In this chapter, we shall describe a few examples of wave modes in fluids, chosen to illustrate general wave properties. As secondary goals of this chapter, we shall also derive some of the principal properties of rotating fluids and of surface tension.

The most familiar types of wave are probably gravity waves on a large body of water (Sec. 15.2), e.g. ocean waves and waves on the surfaces of lakes and rivers. We consider these in the linear approximation and find that they are dispersive in general, though they become nondispersive in the long wavelength limit. We shall illustrate gravity waves by their roles in *helioseismology*, the study of coherent-wave modes excited within the body of the sun by convective overturning motions. We shall also examine the effects of surface tension on gravity waves, and in this connection shall develop a mathematical description of surface tension.

In contrast to the elastodynamic waves of Chap. 11, waves in fluids often develop amplitudes large enough that nonlinear effects become important (Sec. 15.3). It then is not adequate to describe the waves in terms of small perturbations about some stationary state. It turns out that, at least under some restrictive conditions, nonlinear waves have some very surprising properties. In particular there exist *soliton* or *solitary-wave* modes in which the influence of nonlinearity is held in check by dispersion, and particular wave profiles are quite robust and can propagate for long intervals of time. We shall demonstrate this by studying flow in a shallow channel. We shall also explore the remarkable behaviors of such solitons when they pass through each other.

Rotating fluids introduce yet more novel properties (Sec. 15.4), particularly those associated with the Coriolis force. In Sec. 15.4 we show how relatively simple principles find immediate application in analyzing the influence of the Earth's rotation on ocean currents. We also show how to model a viscous boundary layer in the presence of strong rotation. These preliminaries enable us to discuss Rossby waves, for which the restoring force is the Coriolis effect, and which have the unusual property that their group and phase velocities are oppositely directed. Rossby waves are important in both the oceans and the atmosphere.

The simplest fluid waves of all are probably small-amplitude sound waves—a paradigm for scalar waves. These are nondispersive, just like electromagnetic waves, and are therefore sometimes useful for human communication. We shall study sound waves in Sec.15.5 and shall use them to explain how waves can be produced by fluid flows. This will be illustrated with the problem of sound generation by high-speed turbulent flows—a problem that provides a good starting point for the topic of the following chapter, compressible flows.

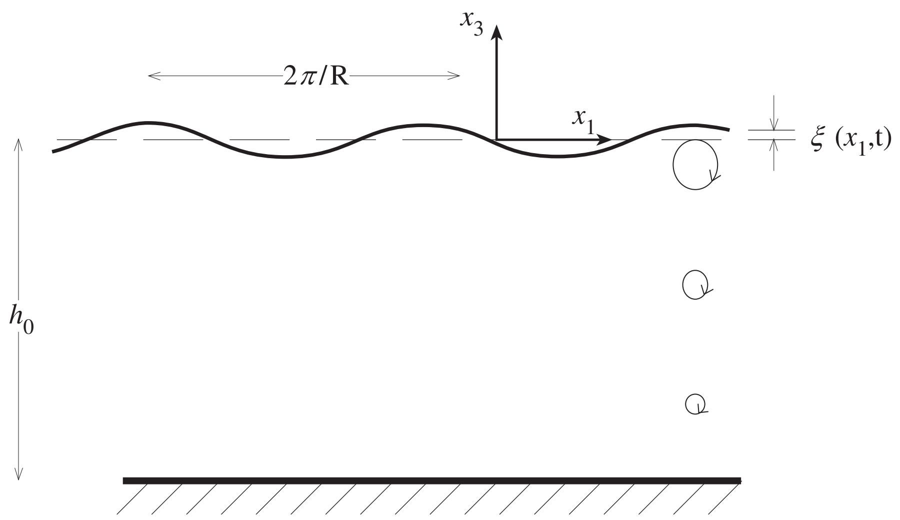

Fig. 15.1: Gravity Waves propagating horizontally across a lake of depth h_o.

15.2 Gravity Waves

Gravity waves[1] are waves on and beneath the surface of a fluid, for which the restoring force is the downward pull of gravity. Familiar examples are ocean waves and the waves produced on the surface of a pond when a pebble is thrown in. Less familiar are "g-modes" of vibration of the sun, discussed at the end of this section.

Consider a small-amplitude wave propagating along the surface of a flat-bottomed lake with depth h_o, as shown in Fig. 15.1. As the water's displacement is small, we can describe the wave as a linear perturbation about equilibrium. The equilibrium water is at rest, i.e.

[1]Not to be confused with *gravitational waves* which are waves in the gravitational field that propagate at the speed of light and which we shall meet in Chap. 25

$\mathbf{v} = 0$. The water's perturbed motion is essentially inviscid and incompressible, $\nabla \cdot \mathbf{v} = 0$. A simple application of the equation of vorticity transport, Eq. (13.3), assures us that since the water is static and thus irrotational before and after the wave passes, it must also be irrotational within the wave. Therefore, we can describe the wave inside the water by a velocity potential ψ whose gradient is the velocity field,

$$\mathbf{v} = \nabla \psi \; . \tag{15.1}$$

Incompressibility, $\nabla \cdot \mathbf{v} = 0$, applied to this equation, implies that the velocity potential ψ satisfies Laplace's equation

$$\nabla^2 \psi = 0 \tag{15.2}$$

We introduce horizontal coordinates x, y and a vertical coordinate z measured upward from the lake's equilibrium surface (cf. Fig. 15.1), and for simplicity we confine attention to a sinusoidal wave propagating in the x direction with angular frequency ω and wave number k. Then ψ and all other perturbed quantities will have the form $f(z)\exp[i(kx - \omega t)]$ for some function $f(z)$. More general disturbances can be expressed as a superposition of many of these elementary wave modes propagating in various horizontal directions (and in the limit, as a Fourier integral). All of the properties of such superpositions follow straightforwardly from those of our elementary plane-wave mode, so we shall continue to focus on it.

We must use Laplace'e equation (15.2) to solve for the vertical variation, $f(z)$, of the velocity potential. As the horizontal variation at a particular time is $\propto \exp(ikx)$, direct substitution into Eq. (15.2) gives two possible vertical variations, $\psi \propto \exp(\pm kz)$. The precise linear combination of these two forms is dictated by the boundary conditions. The one that we shall need is that the vertical component of velocity $v_z = \partial\psi/\partial z$ vanish at the bottom of the lake ($z = -h_o$). The only combination that can vanish is a sinh function. Its integral, the velocity potential, therefore involves a cosh function:

$$\psi = \psi_0 \cosh[k(z + h_o)] \, \exp[i(kx - \omega t)]. \tag{15.3}$$

An alert reader might note at this point that the *horizontal* velocity does not vanish at the lake bottom, whereas a no-slip condition should apply in practice. In fact, as we discussed in Sec 13.4, a thin, viscous boundary layer along the bottom of the lake will join our potential-flow solution (15.3) to nonslipping fluid at the bottom. We shall ignore the boundary layer under the (justifiable) assumption that it is too thin to affect much of the flow.

Returning to the potential flow, we must also impose a boundary condition at the surface. This can be obtained from Bernoulli's law. The version of Bernoulli's law that we need is that for an irrotational, isentropic, time-varying flow:

$$\mathbf{v}^2/2 + h + \Phi + \partial\psi/\partial t = \text{constant everywhere in the flow} \tag{15.4}$$

[Eqs. (12.39), (12.43)]. We shall apply this law at the surface of the perturbed water. Let us examine each term: (i) The term $\mathbf{v}^2/2$ is quadratic in a perturbed quantity and therefore can be dropped. (ii) The enthalpy $h = u + P/\rho$ (cf. Box 12.1) is a constant since u and ρ are constants throughout the fluid and P is constant on the surface and equal to the atmospheric pressure. [Actually, there will be a slight variation of the surface pressure caused by the varying weight of the air above the surface, but as the density of air is typically $\sim 10^{-3}$ that of water, this is a very small correction.] (iii) The gravitational potential at the fluid surface is $\Phi = g_e\xi$, where $\xi(x,t)$ is the surface's vertical displacement from equilibrium and we ignore a constant.

Bernoulli's law applied at the surface therefore simplifies to give

$$g_e\xi + \frac{\partial\psi}{\partial t} = 0 \, . \tag{15.5}$$

Now, the vertical component of the surface velocity in the linear approximation is just the rate of change of the vertical displacement: $v_z(z=0,t) = d\xi/dt$. Retaining only linear terms, we can replace the convective derivative d/dt by the partial derivative $\partial/\partial t$; and expressing v_z in terms of the velocity potential we then obtain

$$\frac{\partial\xi}{\partial t} = v_z = \frac{\partial\psi}{\partial z} \, . \tag{15.6}$$

Combining this with the time derivative of Eq. (15.5), we obtain an equation for the vertical gradient of ψ in terms of its time derivative:

$$g_e\frac{\partial\psi}{\partial z} = -\frac{\partial^2\psi}{\partial t^2}. \tag{15.7}$$

Finally, substituting Eq. (15.3) into Eq. (15.7), we obtain the dispersion relation for linearized gravity waves:

$$\omega^2 = g_e k \tanh(kh_o) \tag{15.8}$$

How do the individual elements of fluid move in a gravity wave? We can answer this question by first computing the vertical and horizontal components of the velocity by differentiating Eq. (15.3). We find that the fluid elements undergo elliptical motion similar to that found for Rayleigh waves on the surface of a solid (Sec.11.5). However, in gravity waves, the sense of rotation of the particles is always the same at a particular phase of the wave, in contrast to reversals found in Rayleigh waves. XXXXKIP: CHECKXXXX

We now consider two limiting cases: deep water and shallow water.

15.2.1 Deep Water Waves

When the water is deep compared to the wavelength of the waves, $kh_o \gg 1$, the dispersion relation (15.8) is approximately

$$\omega = \sqrt{g_e k} \, . \tag{15.9}$$

Thus, deep water waves are dispersive; their group velocity $V_g \equiv d\omega/dk = \frac{1}{2}\sqrt{g_e/k}$ is half their phase velocity, $V_\phi \equiv \omega/k = \sqrt{g_e/k}$. [Note: We could have deduced the deep-water dispersion relation (15.9), up to a dimensionless multiplicative constant, by dimensional arguments: The only frequency that can be constructed from the relevant variables g_e, k, ρ is $\sqrt{g_e k}$.]

15.2.2 Shallow Water Waves

For shallow water waves, with $kh_o \ll 1$, the dispersion relation (15.8) becomes

$$\omega = \sqrt{g_e h_o}\, k \,. \tag{15.10}$$

Thus, these waves are nondispersive; their phase and group velocities are $V_\phi = V_g = \sqrt{g_e h_o}$.

Below, when studying solitons, we shall need two special properties of shallow water waves. First, when the depth of the water is small compared with the wavelength, but not very small, the waves will be slightly dispersive. We can obtain a correction to Eq. (15.10) by expanding the tanh function of Eq. (15.8) as $\tanh x = x - x^3/3 + \ldots$. The dispersion relation then becomes

$$\omega = \sqrt{g_e h_o}\, k \left(1 - \frac{1}{6}k^2 h_o^2\right) \,. \tag{15.11}$$

Second, by computing $v_x = \partial\psi/\partial x$ from Eq. (15.3), we find that the horizontal motion of the fluid is essentially independent of depth in the shallow-water limit.

15.2.3 Capillary Waves

When the wavelength is very short, we must include the effects of *surface tension* on the surface boundary condition. This can be done by a very simple, heuristic argument. Surface tension is usually treated as a force per unit length, γ, that lies in the surface and is unaffected by changes in the shape or size of the surface; see Ex. 15.1. In the case of a gravity wave, this tension produces on the fluid's surface a net downward force per unit area $-\gamma d^2\xi/dx^2 = \gamma k^2 \xi$, where k is the horizontal wave number. [This downward force is like that on a curved violin string; cf. Eq. (11.32) and associated discussion.] This additional force must be included in Eq. (15.5) as an augmentation of ρg_e. Correspondingly, the effect of surface tension on a mode with wave number k is simply to change the true gravity to an *effective gravity*

$$g_e \to g_e + \frac{\gamma k^2}{\rho} \,. \tag{15.12}$$

The remainder of the derivation of the dispersion relation for deep gravity waves carries over unchanged, and it becomes

$$\omega^2 = g_e k + \frac{\gamma k^3}{\rho} \tag{15.13}$$

[Eqs. (15.9) and (15.12)]. When the second term dominates, the waves are sometimes called *capillary waves.*

15.2.4 Helioseismology

The sun provides an excellent example of the excitation of small amplitude waves in a fluid body. In the 1960s, Robert Leighton and colleagues discovered that the surface of the sun oscillate vertically with a period of roughly five minutes and a speed of ~ 1 km s^{-1}. This was thought to be an incoherent surface phenomenon until it was shown that the observed variation was, in fact, the superposition of thousands of highly coherent wave modes excited within the solar cavity — normal modes of the sun. Present day techniques allow surface velocity amplitudes as small as 2 mm s^{-1} to be measured, and phase coherence for intervals as long as a year has been observed. Studying the frequency spectrum and its variation provides a unique probe of the sun's interior structure, just as the measurement of conventional seismic waves, as described in Sec.11.5, probes the earth's interior.

The description of the normal modes of the sun requires some modification of our treatment of gravity waves. We shall eschew details and just outline the principals. First, the sun is (very nearly) spherical! We therefore work in spherical polar coordinates rather than Cartesian coordinates. Second, the sun is made of hot gas and it is no longer a good approximation to assume that the fluid is always incompressible. We must therefore replace the equation $\nabla \cdot \mathbf{v} = 0$ with the full equation of continuity (mass conservation) together with the equation of energy conservation which governs the relationship between the density and pressure perturbations. Third, the sun is not uniform. The pressure and density in the unperturbed gas vary in a known manner and must be included. Fourth, the sun has a finite surface area. Instead of assuming that there will be a continuous spectrum of waves, we must now anticipate that the boundary conditions will lead to a discrete spectrum of normal modes. Allowing for these complications, it is possible to derive a differential equation to replace Eq. (15.7). It turns out that a convenient dependent variable is the pressure perturbation. The boundary conditions are that the displacement vanish at the center of the sun and that the pressure perturbation vanish at the surface.

At this point the problem is reminiscent of the famous solution for the eigenfunctions of the Schrödinger equation for a hydrogen atom in terms of associated Laguerre polynomials. The wave frequencies of the sun's normal modes are given by the eigenvalues of the differential equation. The corresponding eigenfunctions can be classified using three quantum numbers, n, l, m, where n counts the number of radial nodes in the eigenfunction and the angular variation is proportional to the spherical harmonic $Y_l^m(\theta, \phi)$. If the sun were precisely spherical, the modes that are distinguished only by their m quantum number would be degenerate just as is the case with an atom when there is no preferred direction in space. However, the sun rotates with a latitude-dependent period in the range $\sim 25 - 30$d and this breaks the degeneracy just as an applied magnetic field in an atom breaks the degeneracy of the atom's states (the Zeeman effect). From the splitting of the solar-mode spectrum, it is possible to learn about the distribution of rotational angular momentum inside the sun.

When this problem is solved in detail, it turns out that there are two general classes of modes. One class is similar to gravity waves, in the sense that the forces which drive the gas's motions are produced primarily by gravity (either directly, or indirectly via the weight of overlying material producing pressure that pushes on the gas.) These are called *g modes*. In the second class (known as *p* and *f modes*), the pressure forces arise mainly from the compression of the fluid just like in sound waves (which we shall study in Sec. 15.5 below). Now, it turns out that the g modes have large amplitudes in the middle of the sun, whereas the p and f modes are dominant in the outer layers [cf. Fig. 15.2(b)]. The reasons for this are relatively easy to understand and introduce ideas to which we shall return:

The sun is a hot body, much hotter at its center ($T \sim 1.5 \times 10^7$ K) than on its surface ($T \sim 6000$ K). The sound speed c is therefore much greater in its interior and so p and f

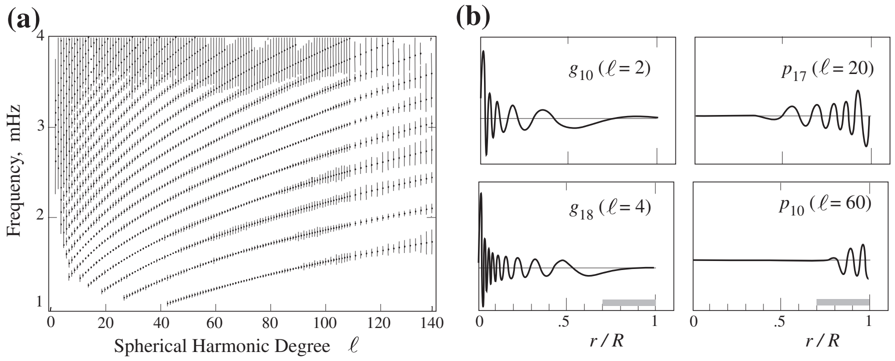

Fig. 15.2: (a) Measured frequency spectrum for solar p-modes with different values of the quantum numbers n, l. The error bars are magnified by a factor 1000. Frequencies for modes with $n > 30$ and $l > 1000$ have been measured. (b) Sample eigenfunctions for g and p modes labeled by n (subscripts) and l (parentheses). The ordinate is the radial velocity and the abscissa is fractional radial distance from the sun's center to its surface. The solar convection zone is the dashed region at the bottom. (Adapted from Libbrecht and Woodard 1991.)

modes of a given frequency ω can carry their energy flux $\sim \rho\xi^2\omega^2 c$ (Sec.15.5) with much smaller amplitudes ξ than near the surface. That is why the $p-$ and $f-$ mode amplitudes are much smaller in the center of the sun than near the surface.

The g-modes are controlled by different physics and thus behave differently: The outer $\sim$ 30 percent (by radius) of the sun is *convective* (cf. Sec. 17.5) because the diffusion of photons is inadequate to carry the huge amount of nuclear energy being generated in the solar core. The convection produces an equilibrium variation of pressure and density with radius that are just such as to keep the sun almost neutrally stable, so that regions that are slightly hotter (cooler) than their surroundings will rise (sink) in the solar gravitational field. Therefore there cannot be a mechanical restoring force which would cause these regions to oscillate about their average positions, and so the g modes (which are influenced almost solely by gravity) have little restoring force and thus are *evanescent* in the convection zone, and so their amplitudes decay quickly with increasing radius there.

We should therefore expect only p and f modes to be seen in the surface motions and this is, indeed the case. Furthermore, we should not expect the properties of these modes to be very sensitive to the physical conditions in the core. A more detailed analysis bears this out.

****

EXERCISES

Exercise 15.1 *Example: Surface Tension*
Consider an arbitrary point $\mathcal{P}$ on a fluid's surface and there set up an orthonormal basis $\mathbf{e}_x, \mathbf{e}_y, \mathbf{e}_z$, with $\mathbf{e}_z$ oriented normal to the surface. Set up local Cartesian coordinates x, y, z with origin at $\mathcal{P}$ and with $\mathbf{e}_j$ pointing along the coordinates' j direction. (These coordinates should not be confused with those of the above gravity-wave analysis.) The unbalanced

intermolecular forces at the fluid's surface produce *surface tension*—i.e., a compressive force per unit length γ lying in the surface.

(a) Show that the associated stress tensor is

$$\mathbf{T} = -\gamma\delta(z)(\mathbf{g} - \mathbf{e}_z \otimes \mathbf{e}_z) \ . \tag{15.14}$$

(Note that $\mathbf{g} - \mathbf{e}_z \otimes \mathbf{e}_z$ is the surface's 2-dimensional metric.)

(b) Let the equation of the surface in the vicinity of $\mathcal{P}$ be $z = x^2/2R_1 + y^2/2R_2$. Show that stress balance $\boldsymbol{\nabla} \cdot \mathbf{T} = 0$ implies that the pressure difference across the surface is

$$\Delta P = \gamma \left(\frac{1}{R_1} + \frac{1}{R_2} \right) \ . \tag{15.15}$$

(R_1 and R_2 are called the surface's "principal radii of curvature" at $\mathcal{P}$.)

Exercise 15.2 *Problem: Capillary Waves*
Consider deep-water gravity waves of short enough wavelength that surface tension must be included, so the dispersion relation is Eq. (15.13). Show that there is a minimum value of the group velocity and find its value together with the wavelength of the associated wave. Evaluate these for water ($\gamma \sim 0.07$ N m^{-1}). Try performing a crude experiment to verify this phenomenon.

Exercise 15.3 *Example: Ship Waves*
Consider the wave pattern produced by a toy boat which moves with uniform velocity $\mathbf{u}$ across a deep pond. Gravity waves and surface tension or *capillary* waves are excited. Show that capillary waves are found both ahead of and behind the boat, and gravity waves, solely in a trailing wedge. More specifically:

(a) In the rest frame of the water, the waves' dispersion relation is Eq. (15.13). Change notation so ω is the waves' angular velocity as seen in the boat's frame and ω_o in the water's frame, so the dispersion relation is $\omega_o^2 = g_e k + (\gamma/\rho)k^3$. Use the doppler shift to derive the boat-frame dispersion relation $\omega(k)$. The boat radiates a spectrum of waves in all directions. However, only those with vanishing frequency in the boat's frame, $\omega = 0$, contribute to the stationary pattern, and they must propagate away from the boat at the group velocity as seen in the water's frame $V_{\rm go}$.

(b) Prove that the stationary wave pattern in any direction θ (cf. Fig. 15.3) is composed of waves whose wave vectors (characterized by k and ϕ) satisfy

$$\tan\theta = \frac{V_{go}(k)\sin\phi}{u + V_{go}\cos\phi} \ , \quad \omega_0(k) = -uk\cos\phi \ . \tag{15.16}$$

Here ω_o, V_{go} are the frequency and group velocity respectively measured in the rest frame of the water. (You may assume that only forward directed waves ($\pi/2 < \phi < 3\pi/2$) can interfere and contribute to the pattern.)

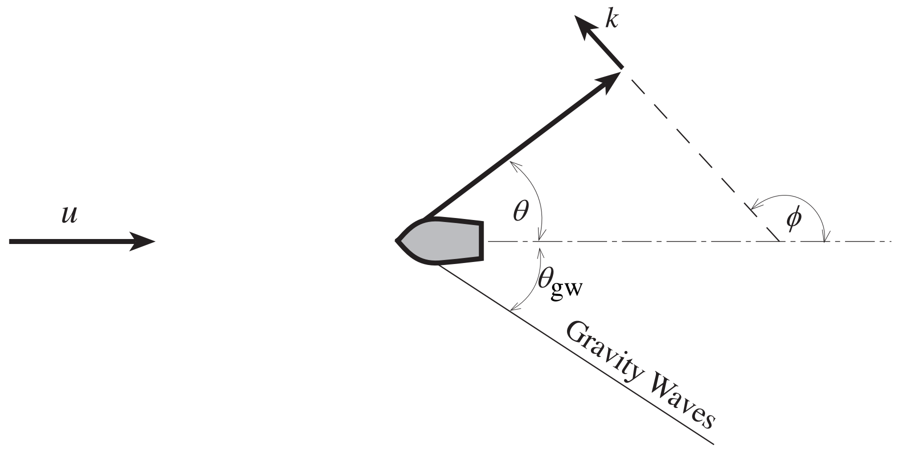

Fig. 15.3: Capillary and Gravity waves excited by a small boat (Ex. 15.3). We denote location in the wave pattern by the angle θ and the direction of the wave vector there, relative to $\mathbf{u}$, by the angle ϕ.

(c) Specialize to capillary waves [$k \gg \sqrt{g_e \rho / \gamma}$]. Show that

$$\tan\theta = \frac{3\tan\phi}{1 - 2\tan^2\phi} \,. \tag{15.17}$$

Demonstrate that the capillary wave pattern is present for all values of θ. Next, specialize to gravity waves and show that

$$\tan\theta = \frac{-\tan\phi}{1 + 2\tan^2\phi} \,. \tag{15.18}$$

Demonstrate that the gravity-wave pattern is confined to a trailing wedge, whose opening angle is $\theta_{\rm gw} = 2\sin^{-1}(1/3) = 38.94^{\rm o}$; cf. Fig. 15.3. You might try to reproduce these results experimentally.

Exercise 15.4 *Example: Breaking of a Dam*
Consider the flow of water along a horizontal channel of constant width after a dam breaks. Sometime after the initial transients have died away, the flow may be described by the nonlinear shallow wave equations, which can be re-expressed in the following form [see Eqs. (15.23) and (15.24) below]

$$\begin{aligned} \frac{\partial h}{\partial t} + \frac{\partial (hv)}{\partial x} &= 0 \,, \\ \frac{\partial v}{\partial t} + v\frac{\partial v}{\partial x} + g_e \frac{\partial h}{\partial x} &= 0 \,. \end{aligned}$$

Here h is the height of the flow, v is the horizontal speed of the flow and x is distance along the channel measured from the location of the dam. The first equation is mass conservation; the second is horizontal momentum conservation. Solve for the flow by assuming that at

$t = 0$, $h = h_o H(-x)$, with $H(\zeta)$ being the step function. What is the speed of the front of the water? [*Hints:* Note that from the parameters of the problem we can construct only one velocity, $\sqrt{g_e h_o}$ and no length. It therefore is a reasonable guess that the solution depends on the single similarity variable

$$\xi = \frac{x/t}{\sqrt{g_e h_o}} . \tag{15.19}$$

Then convert the two partial differential equations above into a pair of ordinary differential equations which can be solved so as to satisfy the boundary conditions.]

****

15.3 Nonlinear Shallow Water Waves and Solitons

In recent decades, *solitons* or solitary waves have been studied intensively in many different areas of physics. However, fluid dynamicists became familiar with them in the nineteenth century. In an oft-quoted pasage, John Scott-Russell described how he was riding along a narrow canal and watched a boat stop abruptly. This deceleration launched a single smooth pulse of water which he followed on horseback for one or two miles, observing it "rolling on a rate of some eight or nine miles an hour, preserving its original figure some thirty feet long and a foot to a foot and a half in height". This was a soliton – a one dimensional, nonlinear wave with fixed profile traveling with constant speed. Solitons can be observed fairly readily when gravity waves are produced in shallow, narrow channels. We shall use the particular example of a shallow, nonlinear gravity wave to illustrate solitons in general.

15.3.1 Korteweg-de Vries (KdV) Equation

The key to a soliton's behavior is a robust balance between the effects of dispersion and the effects of nonlinearity. When one grafts these two effects onto the wave equation for shallow water waves, then at leading order in the strengths of the dispersion and nonlinearity one gets the *Korteweg-de Vries* (KdV) equation for solitons. Since a completely rigorous derivation of the KdV equation is quite lengthy, we shall content ourselves with a somewhat heuristic derivation that is based on this grafting process, and is designed to emphasize the equation's physical content.

We choose as the dependent variable in our wave equation the height ξ of the water's surface above its quiescent position, and we confine ourselves to a plane wave that propagates in the horizontal x direction so $\xi = \xi(x,t)$.

In the limit of very weak waves, $\xi(x,t)$ is governed by the shallow-water dispersion relation $\omega = \sqrt{g_e h_o}\, k$, where h_o is the depth of the quiescent water. This dispersion relation implies that $\xi(x,t)$ must satisfy the following elementary wave equation:

$$0 = \frac{\partial^2 \xi}{\partial t^2} - g_e h_o \frac{\partial^2 \xi}{\partial x^2} = \left(\frac{\partial}{\partial t} - \sqrt{g_e h_o} \frac{\partial}{\partial x} \right) \left(\frac{\partial}{\partial t} + \sqrt{g_e h_o} \frac{\partial}{\partial x} \right) \xi . \tag{15.20}$$

In the second expression, we have factored the wave operator into two pieces, one that governs waves propagating rightward, and the other leftward. To simplify our derivation and the final wave equation, we shall confine ourselves to rightward propagating waves, and correspondingly we can simply remove the left-propagation operator from the wave equation, obtaining

$$\frac{\partial \xi}{\partial t} + \sqrt{g_e h_o}\frac{\partial \xi}{\partial x} = 0 \; . \tag{15.21}$$

(Leftward propagating waves are described by this same equation with a change of sign.)

We now graft the effects of dispersion onto this rightward wave equation. The dispersion relation, including the effects of dispersion at leading order, is $\omega = \sqrt{g_e h_o}\, k(1 - \frac{1}{6}k^2 h_o^2)$ [Eq. (15.11)]. Now, this dispersion relation ought to be derivable by assuming a variation $\xi \propto \exp[i(kx - \omega t)]$ and substituting into a generalization of Eq. (15.21) with corrections that take account of the finite depth of the channel. We will take a short cut and reverse this process to obtain the generalization of Eq. (15.21) from the dispersion relation. The result is

$$\frac{\partial \xi}{\partial t} + \sqrt{g_e h_o}\,\frac{\partial \xi}{\partial x} = -\frac{1}{6}\sqrt{g_e h_o}\; h_o^2 \frac{\partial^3 \xi}{\partial x^3} \; , \tag{15.22}$$

as a direct calculation confirms. This is the "linearized KdV equation". It incorporates weak dispersion associated with the finite depth of the channel but is still a linear equation, only useful for small-amplitude waves.

Now let us set aside the dispersive correction and tackle nonlinearity. For this purpose we return to first principles for waves in very shallow water. Let the height of the surface above the lake bottom be $h = h_o + \xi$. Since the water is very shallow, the horizontal velocity, $v \equiv v_x$, is almost independent of depth (aside from the boundary layer which we ignore); cf. discussion the following Eq. (15.11). The flux of water mass, per unit width of channel, is therefore $\rho h v$ and the mass per unit width is ρh. The law of mass conservation therefore takes the form

$$\frac{\partial h}{\partial t} + \frac{\partial (hv)}{\partial x} = 0 \; , \tag{15.23}$$

where we have canceled the constant density. This equation contains a nonlinearity in the product hv. A second nonlinear equation for h and v can be obtained by differentiating Bernoulli's law (15.5):

$$\frac{\partial v}{\partial t} + v\frac{\partial v}{\partial x} + g_e \frac{\partial h}{\partial x} = 0 \; . \tag{15.24}$$

(This is actually just the x-component of the Euler equation, i.e. momentum conservation, with pressure expressed in the hydrostatic form $P = \rho g_e h$.) Equations (15.23) and (15.24) can be combined to obtain

$$\frac{\partial \left(v - 2\sqrt{g_e h}\right)}{\partial t} + \left(v - \sqrt{g_e h}\right)\frac{\partial \left(v - 2\sqrt{g_e h}\right)}{\partial x} = 0 \; . \tag{15.25}$$

This equation shows that the quantity $v - 2\sqrt{g_e h}$ is constant along characteristics that propagate with speed $v - \sqrt{g_e h}$. (This constant quantity is a special case of a "Riemann invariant", a concept that we shall study in Chap. 16.) When, as we shall require below, the nonlinearites are modest so h does not differ greatly from h_o, these characteristics propagate

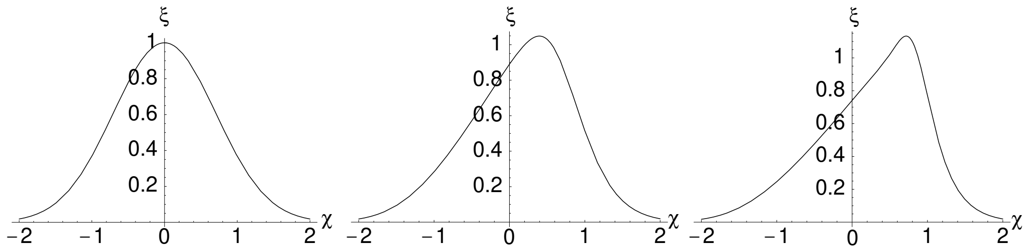

Fig. 15.4: Steepening of a Gaussian wave profile by the nonlinear term in the KdV equation. The increase of wave speed with amplitude causes the leading part of the profile to steepen with time and the trailing part to flatten. In the full KdV equation, this effect can be balanced by the effect of dispersion, which causes the high-frequency Fourier components in the wave to travel slightly slower than the low-frequency components. This allows stable solitons to form.

leftward, which implies that for rightward propagating waves they begin at early times in undisturbed fluid where $v = 0$ and $h = h_o$. Therefore, the constant value of $v - 2\sqrt{g_e h}$ is $-2\sqrt{g_e h_o}$, and correspondingly in regions of disturbed fluid

$$v = 2\left(\sqrt{g_e h} - \sqrt{g_e h_o}\right) . \tag{15.26}$$

Substituting this into Eq. (15.23), we obtain

$$\frac{\partial h}{\partial t} + \left(3\sqrt{g_e h} - 2\sqrt{g_e h_o}\right)\frac{\partial h}{\partial x} = 0 . \tag{15.27}$$

We next substitute $\xi = h - h_o$ and expand to second order in ξ to obtain the final form of our wave equation with nonlinearities but no dispersion:

$$\frac{\partial \xi}{\partial t} + \sqrt{g_e h_o}\frac{\partial \xi}{\partial x} = -\frac{3\xi}{2}\sqrt{\frac{g_e}{h_o}}\frac{\partial \xi}{\partial x} , \tag{15.28}$$

where the term on the right hand side is the nonlinear correction.

We now have separate dispersive corrections (15.22) and nonlinear corrections (15.28) to the rightward wave equation (15.21). Combining the two corrections into a single equation, we obtain

$$\frac{\partial \xi}{\partial t} + \sqrt{g_e h_o}\left[\left(1 + \frac{3\xi}{2h_o}\right)\frac{\partial \xi}{\partial x} + \frac{h_o^2}{6}\frac{\partial^3 \xi}{\partial x^3}\right] = 0 . \tag{15.29}$$

Finally, we substitute

$$\chi \equiv x - \sqrt{g_e h_o}\, t \tag{15.30}$$

to transform into a frame moving rightward with the speed of small-amplitude gravity waves. The result is the full *Korteweg-deVries* or KdV equation:

$$\frac{\partial \xi}{\partial t} + \frac{3}{2}\sqrt{\frac{g_e}{h_o}}\left(\xi\frac{\partial \xi}{\partial \chi} + \frac{1}{9}h_o^3\frac{\partial^3 \xi}{\partial \chi^3}\right) = 0 . \tag{15.31}$$

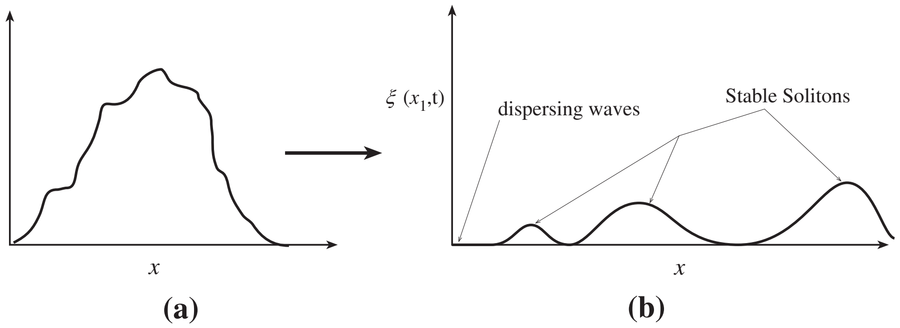

Fig. 15.5: Production of stable solitons out of an irregular initial wave profile.

15.3.2 Physical Effects in the kdV Equation

Before exploring solutions to the KdV equation (15.31), let us consider the physical effects of its nonlinear and dispersive terms. The second, nonlinear term derives from the nonlinearity in the $(\mathbf{v}\cdot\nabla)\mathbf{v}$ term of the Navier-Stokes equation. The effect of this nonlinearity is to steepen the leading edge of a wave profile and flatten the trailing edge (Fig. 15.4.) Another way to understand the effect of this term is to regard it as a nonlinear coupling of linear waves. Since it is nonlinear in the wave amplitude, it can couple together waves with different wave numbers k. For example if we have a purely sinusoidal wave $\propto \exp(ikx)$, then this nonlinearity will lead to the growth of a first harmonic $\propto \exp(2ikx)$. Similarly, when two linear waves with spatial frequencies k, k' are superposed, this term will describe the production of new waves at the sum and difference spatial frequencies. We have already met such wave-wave coupling in our study of nonlinear optics (Chap. 9), and in the route to turbulence for rotating Couette flow (Fig. 14.12), and we shall meet it again in nonlinear plasma physics (Chap. 22).

The third term in (15.31) is linear and is responsible for a weak dispersion of the wave. The higher-frequency Fourier components travel with slower phase velocities than lower-frequency components. This has two effects. One is an overall spreading of a wave in a manner qualitatively familiar from elementary quantum mechanics; cf. Ex. 6.2. For example, in a Gaussian wave packet with width Δx, the range of wave numbers k contributing significantly to the profile is $\Delta k \sim 1/\Delta x$. The spread in the group velocity is then $\sim \Delta k\, \partial^2\omega/\partial k^2 \sim (g_e/h_o)^{1/2} h_o^2\, k\Delta k$. The wave packet will then double in size in a time

$$t_{spread} \sim \frac{\Delta x}{\Delta v_g} \sim \left(\frac{\Delta x}{h_o}\right)^2 \frac{1}{\sqrt{g_e h_o}}. \tag{15.32}$$

The second effect is that since the high-frequency components travel somewhat slower than the low-frequency components, there will be a tendency for the profile to become asymmetric with the trailing edge steeper than the leading edge.

Given the opposite effects of these two corrections (nonlinearity makes the wave's leading edge steeper; dispersion reduces its steepness), it should not be too surprising in hindsight that it is possible to find solutions to the KdV equation with constant profile, in which nonlinearity balances dispersion. What is quite surprising, though, is that these solutions, called *solitons*, are very robust and arise naturally out of random initial data. That is to say,

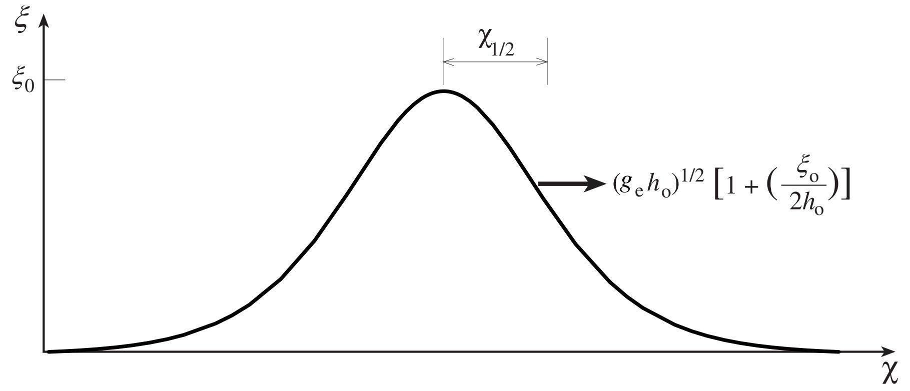

Fig. 15.6: Profile of the single-soliton solution (15.35), (15.33) of the KdV equation. The width $\chi_{1/2}$ is inversely proportional to the square root of the peak height ξ_o.

if we solve an initial value problem numerically starting with several peaks of random shape and size, then although much of the wave will spread and disappear due to dispersion, we will typically be left with several smooth soliton solutions, as in Fig. 15.5.

15.3.3 Single-Soliton Solution

We can discard some unnecessary algebraic luggage in the KdV equation (15.31) by transforming both independent variables using the substitutions

$$\zeta = \frac{\xi}{h_o}\,, \quad \eta = \frac{3\chi}{h_o}\,, \quad \tau = \frac{9}{2}\sqrt{\frac{g_e}{h_o}}\,t\,. \tag{15.33}$$

The KdV equation then becomes

$$\frac{\partial\zeta}{\partial\tau} + \zeta\frac{\partial\zeta}{\partial\eta} + \frac{\partial^3\zeta}{\partial\eta^3} = 0 \tag{15.34}$$

There are well understood mathematical techniques[2] for solving equations like the KdV equation. However, we shall just quote solutions and explore their properties. The simplest solution to the dimensionless KdV equation (15.34) is

$$\zeta = \zeta_0 \mathrm{sech}^2\left[\left(\frac{\zeta_0}{12}\right)^{1/2}\left(\eta - \frac{1}{3}\zeta_0\tau\right)\right]\,. \tag{15.35}$$

This solution describes a one-parameter family of stable solitons. Since the peak amplitude of the wave is $\xi_o = h_o\zeta_0$, the speed of propagation is related to the peak amplitude by

$$\frac{dx}{dt} = \sqrt{g_e h_o}\left[1 + \left(\frac{\xi_o}{2h_o}\,.\right)\right] \tag{15.36}$$

[2]See, for example, Whitham (1974).

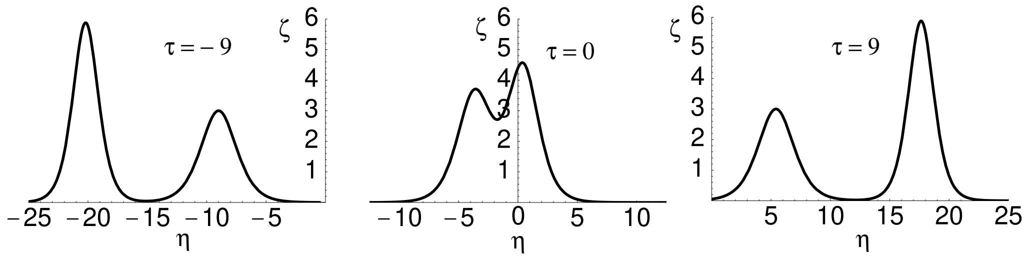

Fig. 15.7: Two-Soliton solution to the dimensionless KdV equation (15.34). This solution describes two waves well separated for $\tau \to -\infty$ that coalesce and then separate producing the original two waves in reverse order as $\tau \to +\infty$. The notation is that of Eq. (15.38); the values of the parameters in that equation are $\eta_1 = \eta_2 = 0$ (so the solitons will be merged at time $\eta = 0$), $\alpha_1 = 1$, $\alpha_2 = 1.4$.

The first term is the propagation speed of a linear wave. The second term is the nonlinear correction, proportional to the wave amplitude ξ_o. The half width of the wave may be defined by setting the argument of the hyperbolic secant to unity:

$$\chi_{1/2} = \left(\frac{4h_o^3}{3\xi_o}\right)^{1/2} . \tag{15.37}$$

The larger the wave amplitude, the narrower its length and the faster it propagates; cf. Fig. 15.6.

Let us return to Scott-Russell's soliton. Converting to SI units, the speed was about 4 m s^{-1} giving an estimate of the depth of the canal as $h_o \sim 1.6$ m. Using the width $\chi_{1/2} \sim 5$ m, we obtain a peak height $\xi_o \sim 0.25$ m, somewhat smaller than quoted but within the errors allowing for the uncertainty in the definition of the width and an (appropriate) element of hyperbole in the account.

15.3.4 Two-Soliton Solution

One of the most fascinating properties of solitons is the way that two or more waves interact. The expectation, derived from physics experience with weakly-coupled normal modes, might be that if we have two well-separated solitons propagating in the same direction with the larger wave chasing the smaller wave, then the larger will eventually catch up with the smaller and nonlinear interactions between the two waves will essentially destroy both, leaving behind a single, irregular pulse which will spread and decay after the interaction. However, this is not what happens. Instead, the two waves pass through each other unscathed and unchanged, except that they emerge from the interaction a bit sooner than they would have had they moved with their original speeds during the interaction. See Fig. 15.7. We do not have time to explain why the two waves survive unscathed, save to remark that there are topological invariants in the solution which have to be preserved. However, we can exhibit one such two-soliton solution analytically:

$$\zeta = \frac{\partial^2}{\partial \eta^2}[12 \ln F(\eta, \tau)] ,$$

$$\text{where } F = 1 + f_1 + f_2 + \left(\frac{\alpha_2 - \alpha_1}{\alpha_2 + \alpha_1}\right)^2 f_1 f_2 \;,$$
$$\text{and } f_i = \exp[-\alpha_i(\eta - \eta_i) + \alpha_i^3 \tau] \;; \tag{15.38}$$

here α_i and η_i are constants. This solution is depicted in Fig. 15.7.

****

EXERCISES

Exercise 15.5 *Derivation: Single-Soliton Solution*
Verify that expression (15.35) does indeed satisfy the dimensionless KdV equation (15.33).

Exercise 15.6 *Derivation: Two-Soliton Solution*

(a) Verify, using symbolic-manipulation computer software (e.g., Macsyma, Maple or Mathematica) that the two-soliton expression (15.38) satisfies the dimensionless KdV equation. (Warning: Considerable algebraic travail is required to verify this by hand, directly.)

(b) Verify analytically that the two-soliton solution (15.38) has the properties claimed in the text: First consider the solution at early times in the spatial region where $f_1 \sim 1, f_2 \ll 1$. Show that the solution is approximately that of the single-soliton described by Eq. (15.35). Demonstrate that the amplitude is $\zeta_{01} = 3\alpha_1^2\tau$ and find the location of its peak. Repeat the exercise for the second wave and for late times.

(c) Use a computer to follow, numerically, the evolution of this two-soliton solution as time η passes (thereby filling in timesteps between those shown in Fig. 15.7).

****

15.3.5 Solitons in Contemporary Physics

Solitons were re-discovered in the 1960's when they were found in numerical plasma simulations. Their topological properties were soon discovered and general methods to generate solutions were derived. Solitons have been isolated in such different subjects as the propagation of magnetic flux in a Josephson junction, elastic waves in anharmonic crystals, quantum field theory (as *instantons*) and classical general relativity (as solitary, nonlinear gravitational waves). Most classical solitons are solutions to one of a relatively small number of nonlinear ordinary differential equations, including the KdV equation, *Burgers' equation* and the *sine-Gordon* equation. Unfortunately it has proved difficult to generalize these equations and their soliton solutions to two and three spatial dimensions.

Just like research into chaos, studies of solitons have taught physicists that nonlinearity need not lead to maximal disorder in physical systems, but instead can create surprisingly stable, ordered structures.

15.4 Rotating Fluids

Fluids with large-scale rotation, most notably the Earth's oceans and atmosphere, exhibit quite different wave phenomena than nonrotating fluids. Before we analyze our main example, Rossby waves, we must derive some important general properties of flows with large-scale rotation. More specifically, we must develop tools for studying modest deviations from rotation with a uniform angular velocity. This is best done by analyzing the deviations in a rotating reference frame, where the unperturbed fluid is at rest.

15.4.1 Equations of Fluid Dynamics in a Rotating Reference Frame

We wish to transform the Navier-Stokes equation from the inertial frame in which it was derived to a uniformly rotating frame: the mean rest frame of the flows we shall study.

We begin by observing that the Navier-Stokes equation has the same form as Newton's second law for particle motion:

$$\frac{d\mathbf{v}}{dt} = \mathbf{f}, \tag{15.39}$$

where the force per unit mass is $\mathbf{f} = -\boldsymbol{\nabla} P/\rho - \boldsymbol{\nabla}\Phi_e + \nu\nabla^2\mathbf{v}$. We transform to a frame rotating with uniform angular velocity $\boldsymbol{\Omega}$ by adding "fictitious" Coriolis and centrifugal accelerations, given respectively by $-2\boldsymbol{\Omega}\times\mathbf{v}$ and $-\boldsymbol{\Omega}\times(\boldsymbol{\Omega}\times\mathbf{x})$, and expressing the force $\mathbf{f}$ in rotating coordinates. The fluid velocity transforms as

$$\mathbf{v} \to \mathbf{v} + \boldsymbol{\Omega}\times\mathbf{x}. \tag{15.40}$$

It is straightforward to verify that this transformation leaves the expression for the viscous acceleration, $\nu\nabla^2\mathbf{v}$, unchanged. Therefore the expression for the force is unchanged, and the Navier-Stokes equation in rotating coordinates becomes

$$\frac{d\mathbf{v}}{dt} = -\frac{\boldsymbol{\nabla} P}{\rho} - \boldsymbol{\nabla}\Phi_e + \nu\nabla^2\mathbf{v} - 2\boldsymbol{\Omega}\times\mathbf{v} - \boldsymbol{\Omega}\times(\boldsymbol{\Omega}\times\mathbf{x})\ . \tag{15.41}$$

Now, the centrifugal acceleration $-\boldsymbol{\Omega}\times(\boldsymbol{\Omega}\times\mathbf{x})$ can be expressed as the gradient of a centrifugal potential, $\boldsymbol{\nabla}[-\frac{1}{2}(\boldsymbol{\Omega}\times\mathbf{x})^2]$. For simplicity, we shall confine ourselves to an incompressible fluid so that ρ is constant. This allows us to define an *effective pressure*

$$P' = P + \rho\left[\Phi_e + \frac{1}{2}(\Omega\times\mathbf{r})^2\right] \tag{15.42}$$

that includes the combined effects of the real pressure, gravity and the centrifugal force. In terms of P' the Navier-Stokes equation in the rotating frame becomes

$$\frac{d\mathbf{v}}{dt} = -\frac{\boldsymbol{\nabla} P'}{\rho} + \nu\nabla^2\mathbf{v} - 2\boldsymbol{\Omega}\times\mathbf{v}\ . \tag{15.43}$$

The quantity P' will be constant if the fluid is at rest, in contrast to the true pressure P which does have a gradient. Equation (15.43) is the most useful form for the Navier-Stokes equation in a rotating frame.

It should be evident from Eq. (15.43) that two dimensionless numbers characterize rotating fluids. The first is the *Rossby number*,

$$\mathrm{Ro} = \frac{V}{L\Omega} , \tag{15.44}$$

where V is a characteristic velocity of the flow relative to the rotating frame and L is a characteristic length. Ro measures the relative strength of the inertial acceleration and the Coriolis acceleration:

$$\mathrm{Ro} \sim \frac{|(\mathbf{v}\cdot\boldsymbol{\nabla})\mathbf{v}|}{|2\boldsymbol{\Omega}\times\mathbf{v}|} \sim \frac{\text{inertial force}}{\text{Coriolis force}} . \tag{15.45}$$

The second dimensionless number is the *Ekman number*,

$$\mathrm{Ek} = \frac{\nu}{\Omega L^2} , \tag{15.46}$$

which similarly measures the relative strengths of the viscous and Coriolis accelerations:

$$\mathrm{Ek} \sim \frac{|\nu\nabla^2\mathbf{v}|}{|2\boldsymbol{\Omega}\times\mathbf{v}|} \sim \frac{\text{viscous force}}{\text{Coriolis force}} . \tag{15.47}$$

Notice that $\mathrm{Ro}/\mathrm{Ek} = R$ is the Reynolds' number.

The two traditional examples of rotating flows are large-scale storms on the rotating earth, and water in a stirred teacup. For a typical storm, the wind speed might be ~ 25 mph or $V \sim 10$ m s^{-1}, and a characteristic length scale might be ~ 1000 km. The effective angular velocity at a temperate latitude is $\Omega_\star = \Omega_\oplus \sin 45^\circ \sim 10^{-4}$ rad s^{-1}, where $\Omega_\oplus$ is the Earth's angular velocity (cf. the next paragraph). As the air's kinematic viscosity is $\nu \sim 10^{-5}$ m^2 s^{-1}, we find that $\mathrm{Ro} \sim 0.1$ and $\mathrm{Ek} \sim 10^{-13}$. This tells us immediately that rotational effects are important but not dominant in controlling the weather and that viscous boundary layers will be very thin.

For water stirred in a teacup (with parameters typical of many flows in the laboratory), $L \sim 10$ cm, $\Omega \sim V/L \sim 10$ rad s^{-1} and $\nu \sim 10^{-6}$ m^2 s^{-1} giving $\mathrm{Ro} \sim 1$, $\mathrm{Ek} \sim 10^{-5}$. Viscous forces are somewhat more important in this case.

For large-scale flows in the earth's atmosphere or oceans (e.g. storms), the rotation of the unperturbed fluid is that due to rotation of the earth. One might think that this means we should take, as the angular velocity $\boldsymbol{\Omega}$ in the Coriolis term of the Navier-Stokes equation (15.43), the earth's angular velocity $\boldsymbol{\Omega}_\oplus$. Not so. The atmosphere and ocean are so thin vertically that vertical motions cannot achieve small Rossby numbers; i.e. Coriolis forces are unimportant for vertical motions. Correspondingly, the only component of the Earth's angular velocity $\boldsymbol{\Omega}_\oplus$ that is important for Coriolis forces is that which couples horizontal flows to horizontal flows: the vertical component $\Omega_* = \Omega_\oplus \sin(\text{latitute})$. (A similar situation occurs for a Foucault pendulum). Thus, in the Coriolis term of the Navier-Stokes equation we must set $\boldsymbol{\Omega} = \Omega_* \mathbf{e}_z = \Omega_\oplus \sin(\text{latitude})\mathbf{e}_z$, where $\mathbf{e}_z$ is the vertical unit vector. By contrast, in the centrifugal potential $\frac{1}{2}(\boldsymbol{\Omega}\times\mathbf{x})^2$, $\boldsymbol{\Omega}$ rmains the full angular velocity of the Earth, $\boldsymbol{\Omega}_\oplus$.

Uniform rotational flows in a teacup or other vessel also typically have $\boldsymbol{\Omega}$ vertically directed. This will be the case for all flows considered in this section.

15.4.2 Geostrophic Flows

Stationary flows $\partial \mathbf{v}/\partial t = 0$ in which both the Rossby and Ekman numbers are small (i.e. with Coriolis forces big compared to inertial and viscous forces) are called *geostrophic*, even in the laboratory. Geostrophic flow is confined to the bulk of the fluid, well away from all boundary layers, since viscosity will become important in those layers. For such geostrophic flow, the Navier-Stokes equation (15.43) reduces to

$$2\boldsymbol{\Omega} \times \mathbf{v} = -\frac{\boldsymbol{\nabla} P'}{\rho} \ . \tag{15.48}$$

This equation says that the velocity $\mathbf{v}$ (measured in the rotating frame) is orthogonal to the body force $\boldsymbol{\nabla} P'$, which drives it. Correspondingly, the streamlines are perpendicular to the gradient of the generalized pressure; i.e. they lie in the surfaces of constant P'.

An example of geostrophic flow is the motion of atmospheric winds around a low pressure region or *depression*. The geostrophic equation (15.48) tells us that such winds must be counter-clockwise in the northern hemisphere as seen from a satellite, and clockwise in the southern hemisphere. For a flow with speed $v \sim 10$ m s^{-1} around a ~ 1000 km depression, the drop in effective pressure at the depression's center is $\Delta P' \sim 1$ kPa or ~ 10 mbar or ~ 0.01 atmosphere. Around a high-pressure region winds will circulate in the opposite direction.

It is here that we can see the power of introducing the effective pressure P'. In the case of atmospheric and oceanic flows, the true pressure P changes significantly vertically, and the pressure scale height is generally much shorter than the horizontal length scale. However, the effective pressure will be almost constant vertically, any small variation being responsible for minor updrafts and downdrafts which we generally ignore when describing the wind or current flow pattern. It is the horizontal pressure gradients which are responsible for driving the flow. When pressures are quoted, they must therefore be referred to some reference equipotential surface, $\Phi_e + \frac{1}{2}(\boldsymbol{\Omega} \times \mathbf{x})^2 =$constant. The convenient one to use is the equipotential associated with the surface of the ocean, usually called "mean sea level". This is the pressure that appears on a meteorological map.

15.4.3 Taylor-Proudman Theorem

There is a simple theorem due to Taylor and Proudman which simplifies the description of three dimensional, geostrophic flows. Take the curl of Eq. (15.48) and use $\boldsymbol{\nabla} \cdot \mathbf{v} = 0$ for incompressible flow; the result is

$$(\boldsymbol{\Omega} \cdot \nabla)\mathbf{v} = 0. \tag{15.49}$$

Thus, there can be no vertical gradient of the velocity under geostrophic conditions. This result provides a good illustration of the stiffness of vortex lines. The simplest demonstration of this theorem is the Taylor column of Fig. 15.8.

It is easy to see that *any* vertically constant, divergence-free velocity field $\mathbf{v}(x, y)$ can be a solution to the geostrophic equation (15.48). The generalized pressure P' can be adjusted to make it a solution. However, one must keep in mind that to guarantee it is also a true (approximate) solution of the full Navier-Stokes equation (15.43), its Rossby and Ekman numbers must be $\ll 1$.

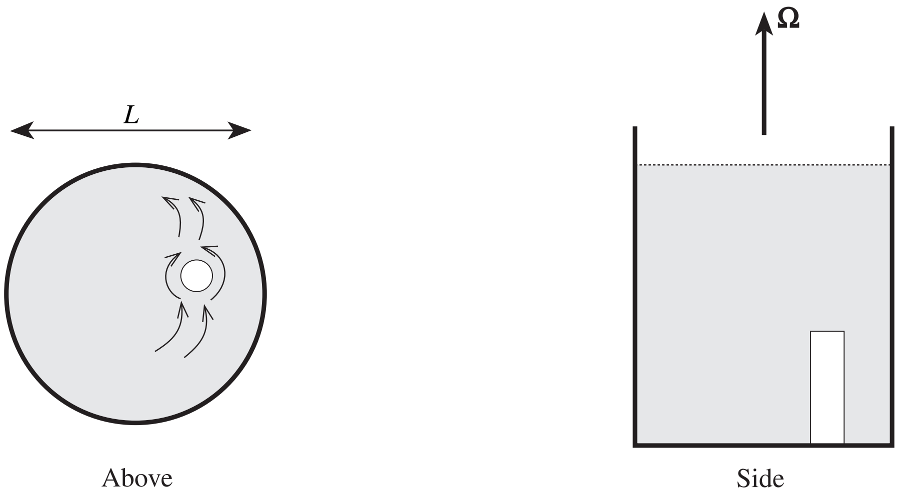

Fig. 15.8: Taylor Column. A solid cylinder is placed in a large container of water which is then spun up on a turntable to a high enough angular velocity Ω that the Ekman number is small, $\mathrm{Ek} = \nu/\Omega L^2 \ll 1$. A slow, steady flow relative to the cylinder is then induced. (The flow's velocity $\mathbf{v}$ in the rotating frame must be small enough to keep the Rossby number $\ll 1$.) The water in the bottom half of the container flows around the cylinder. The water in the top half does the same as if there were an invisible cylinder present. This is an illustration of the Taylor-Proudman theorem which states that there can be no vertical gradients in the velocity field. The effect can also be demonstrated with vertical velocity: If the cylinder is slowly made to rise, then the fluid immediately above it will also be pushed upward rather than flow past the cylinder—except at the water's surface, where the geostrophic flow breaks down. The fluid above the cylinder, which behaves as though it were rigidly attached to the cylinder, is called a Taylor column.

15.4.4 Ekman Pumping

As we have seen, Ekman numbers are typically very small in the bulk of a rotating fluid. However, as was true in the absence of rotation, the no slip condition at a solid surface generates a boundary layer that can indirectly impose a major influence on the global velocity field.

When the Rossby number is small, typically $\lesssim 1$, the structure of a laminar boundary layer is dictated by a balance between viscous and Coriolis forces rather than viscous and inertial forces. Balancing the relevant terms in Eq. (15.43), we obtain an estimate of the boundary-layer thickness:

$$\text{thickness} \sim \delta_E \equiv \sqrt{\frac{\nu}{\Omega}}\,. \tag{15.50}$$

In other words, the thickness of the boundary layer is that which makes the layer's Ekman number unity, $\mathrm{Ek}(\delta_E) = \nu/(\Omega\delta_E^2) = 1$.

Consider such an "Ekman boundary layer" at the bottom or top of a layer of geostrophically flowing fluid. For the same reasons as we met in the case of ordinary laminar boundary layers, the generalized pressure P' will be nearly independent of height z through the Ekman layer; i.e. it will have the value dictated by the flow just outside the layer: $\boldsymbol{\nabla} P' = -2\boldsymbol{\Omega}\times\mathbf{V}\rho$, where $\mathbf{V}$ is the velocity just outside the layer. Since $\boldsymbol{\Omega}$ is vertical, $\boldsymbol{\nabla} P'$ like $\mathbf{V}$ will be hori-

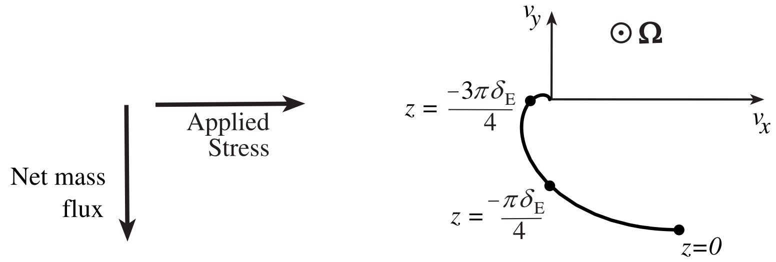

Fig. 15.9: Ekman pumping at a surface where the wind exerts a stress.

zontal, i.e., they will lie in the x, y plane. To simplify the analysis, we introduce a complex velocity field,

$$v \equiv (v_x - V) + iv_y \ . \tag{15.51}$$

Then after some algebra, the Navier-Stokes equation (15.43) with $\boldsymbol{\nabla} P' = -2\boldsymbol{\Omega} \times \mathbf{V}\rho$, takes on the following remarkable form:

$$\frac{d^2 v}{dz^2} = \left(\frac{1+i}{\delta_E}\right)^2 v \tag{15.52}$$

This must be solved subject to some appropriate boundary condition at the water's boundary, and the condition that $\mathbf{v} \to \mathbf{V}$ far from the boundary, i.e., $v \to 0$ there.

For a first illustration of an Ekman layer, consider the effects of a wind blowing in the $\mathbf{e}_x$ direction above a still ocean and orient $\mathbf{e}_z$ vertically upward from the ocean's surface. The wind will exert, through a turbulent boundary layer of air, a stress T_{xz} on the ocean's surface, and this must be balanced by an equal, viscous stress at the top of the water's boundary layer. Thus, there must be a velocity gradient, $dv_x/dz = T_{xz}/\nu\rho$ in the water at $z = 0$. Imposing this boundary condition along with $\mathbf{v} \to 0$ as $z \to -\infty$, we we find from Eqs. (15.52) and (15.51):

$$\begin{aligned} v_x &= \left(\frac{T_{xz}\delta_E}{\sqrt{2}\,\nu\rho}\right) e^{z/\delta_E} \cos(z/\delta_E - \pi/4) \\ v_y &= \left(\frac{T_{xz}\delta_E}{\sqrt{2}\,\nu\rho}\right) e^{z/\delta_E} \sin(z/\delta_E - \pi/4) \end{aligned} \tag{15.53}$$

for $z \le 0$; cf. Fig. 15.9. As a function of depth, this velocity field has the form of a spiral—the so-called Eckman spiral.

By integrating the mass flux $\rho\mathbf{v}$ over z, we find for the total mass flowing per unit time per unit length of the ocean's surface

$$\mathbf{F} = \rho \int_{-\infty}^{0} \mathbf{v} dz = -\frac{T_{xz}}{\nu}\mathbf{e}_y; \tag{15.54}$$

see Fig. 15.9. Thus, the wind, blowing in the $\mathbf{e}_x$ direction, causes a net mass flow in the direction of $\mathbf{e}_x \times \boldsymbol{\Omega}/\Omega = -\mathbf{e}_y$. This response may seem less paradoxical if one recalls how a gyroscope responds to applied forces.

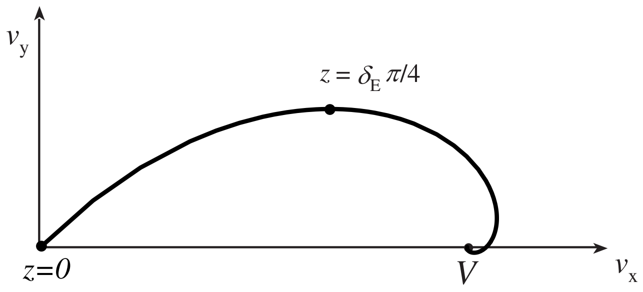

Fig. 15.10: Ekman Spiral: The velocity in the bottom boundary layer when the bulk flow above it moves geostrophically with speed $V\mathbf{e}_x$. .

This mechanism is responsible for the creation of *gyres* in the oceans; cf. Ex. 15.7 and Fig. 15.12.

As a second illustration of an Ekman boundary layer, we consider a geostrophic flow with nonzero velocity $\mathbf{V} = V\mathbf{e}_x$ in the bulk of the fluid, and we examine this flow's interaction with a static, solid surface at its bottom. The structure of the boundary layer on the bottom can be inferred from that of our previous example by adding a constant velocity and a corresponding constant pressure gradient. The resulting solution is

$$v_x = V\exp(-z/\delta_E)\cos(z/\delta_E) \ , \quad v_y = V\exp(-z/\delta_E)\sin(z/\delta_E) \ , \quad v_z = 0 \ . \tag{15.55}$$

This solution, shown in Fig. 15.10, is a second example of the Ekman spiral.

Ekman boundary layers are important because they can circulate rotating fluids faster than viscous diffusion. Suppose we have a nonrotating container (e.g., a tea cup) of radius $\sim L$, containing a fluid that rotates with angular velocity Ω (e.g., due to stirring; cf. Ex. 15.8). As you will see in your analysis of Ex. 15.8, the Eckman layer at the container's bottom experiences a pressure difference between the wall and the container's center given by $\Delta P \sim \rho L^2\Omega^2$. This drives a fluid circulation in the Ekman layer, from the wall toward the center, of magnitude $V \sim \Omega L$. The circulating fluid must upwell at the bottom's center from the Eckman layer into the bulk fluid. This produces a poloidal mixing of the fluid on a timescale given by

$$t_E \sim \frac{L^3}{L\delta_E V} \sim \frac{L\delta_E}{\nu} \ . \tag{15.56}$$

This is shorter than the timescale for simple diffusion of viscosity, $t_V \sim L^2/\nu$ by a factor of order the Rossby number, which as we have seen can be very small. This circulation and mixing are key to the piling up of tea leaves at the bottom center of a stirred tea cup, and to the mixing of the tea or milk into the cup's hot water; cf. Ex. 15.8.

15.4.5 Rossby Waves

Somewhat surprisingly, Coriolis forces can drive wave motion. In the simplest example, we consider the sea above a sloping seabed; see Fig. 15.11. We assume the unperturbed fluid has vanishing velocity $\mathbf{v} = 0$ in the earth's rotating frame, and we study weak waves in the sea with velocity $\mathbf{v}$. (As above, when fluid is at rest in the equilibrium state about which

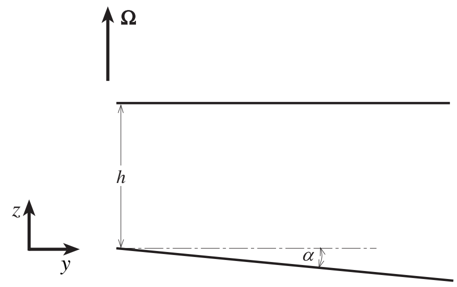

Fig. 15.11: Geometry of ocean for Rossby waves.

we are perturbing, we write the perturbed velocity as $\mathbf{v}$ rather than $\delta\mathbf{v}$.) We also assume that the wavelengths are long enough that viscosity is negligible. We shall also, in this case, restrict attention to small-amplitude waves so that nonlinear terms can be dropped from our dynamical equations. The perturbed Navier-Stokes equation (15.43) then becomes (after linearization)

$$\frac{\partial \mathbf{v}}{\partial t} + 2\mathbf{\Omega} \times \mathbf{v} = \frac{\boldsymbol{\nabla} \delta P'}{\rho} , \tag{15.57}$$

and the linearized equation of mass conservation becomes the incompressibility relation

$$\boldsymbol{\nabla} \cdot \mathbf{v} = 0 . \tag{15.58}$$

Taking the curl of Eq. (15.57), we obtain for the time derivative of the waves' vorticity

$$\frac{\partial \boldsymbol{\omega}}{\partial t} = 2(\mathbf{\Omega} \cdot \nabla)\mathbf{v} . \tag{15.59}$$

We seek a wave mode in which the horizontal fluid velocity oscillates in the x direction, v_x, $v_y \propto \exp[i(kx - \omega t)]$ and is independent of z, in accord with the Taylor-Proudman theorem:

$$v_x \text{ and } v_y \propto \exp[i(kx - \omega t)] , \quad \frac{\partial v_x}{\partial z} = \frac{\partial v_y}{\partial z} = 0 . \tag{15.60}$$

The only allowed vertical variation is in the vertical velocity v_z, and differentiating Eq. (15.58), we obtain

$$\frac{\partial^2 v_z}{\partial z^2} = 0 . \tag{15.61}$$

The vertical velocity therefore varies linearly between the surface and the sea floor. Now, one boundary condition is that the vertical velocity must vanish at the surface. The other is that, at the seafloor $z = -h$, we must have $v_z(-h) = \alpha v_y(x)$, where α is the angle of inclination of the sea floor. The solution to Eq. (15.61) satisfying these boundary conditions is

$$v_z = -\frac{\alpha z}{h} v_y . \tag{15.62}$$

Taking the vertical component of Eq. (15.59) and evaluating $\omega_z = v_{y,x} - v_{x,y} = ikv_y$, we obtain

$$\omega k v_y = 2\Omega \frac{\partial v_z}{\partial z} = \frac{2\Omega \alpha v_y}{h} . \tag{15.63}$$

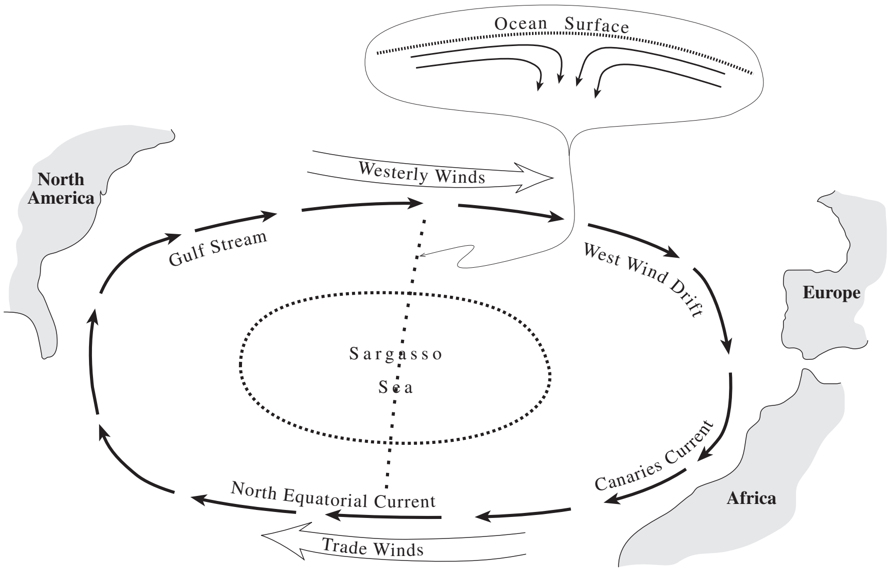

Fig. 15.12: Winds and ocean currents in the north Atlantic. The upper inset shows the surface currents, along the dotted north-south line, that produce the Sargasso-Sea gyre.

The dispersion relation therefore has the quite unusual form

$$\omega k = \frac{2\Omega\alpha}{h} \,. \tag{15.64}$$

Rossby waves have interesting properties: They can only propagate in one direction—parallel to the intersection of the sea floor with the horizontal (our $\mathbf{e}_x$ direction). Their phase velocity $\mathbf{V}_\phi$ and group velocity $\mathbf{V}_g$ are equal in magnitude but in opposite directions,

$$\mathbf{V}_\phi = -\mathbf{V}_g = -\frac{2\Omega\alpha}{k^2 h}\mathbf{e}_x \tag{15.65}$$

If we use (15.58), we discover that the two components of horizontal velocity are in quadrature, $v_x = i\alpha v_y/kh$. This means that, when seen from above, the fluid circulates with the opposite sense to the angular velocity Ω.

Rossby waves in air can be seen as undulations in the atmosphere's jet stream, produced when the stream goes over a sloping terrain such as that of the Rocky Mountains.

****

EXERCISES

Exercise 15.7 *Example: Winds and Ocean Currents in the North Atlantic*
In the north Atlantic Ocean there is the pattern of winds and ocean currents shown in Fig. 15.12. Westerly winds blow from west to east at 40 degrees latitude. Trade winds blow from east to west at 20 degrees latitude. In between, around 30 degrees latitude, is the Sargasso Sea: A 1.5-meter high gyre (raised hump of water). The gyre is created by ocean

surface currents, extending down to a depth of only about 30 meters, that flow northward from the trade-wind region and southward from the westerly wind region; see the upper inset in Fig. 15.12. A deep ocean current, extending from the surface down to near the bottom, circulates around the Sargasso-Sea gyre in a clockwise manner. This current goes under different names in different regions of the ocean: gulf stream, west wind drift, Canaries current, and north equatorial current. Explain both qualitatively and semiquantitatively (in order of magnitude) how the winds are ultimately responsible for all these features of the ocean.

Exercise 15.8 *Example: Circulation in a Tea Cup*
Place tea leaves and water in a tea cup or glass or other container. Stir the water until it is rotating uniformly, and then stand back and watch the motion of the water and leaves. Notice that the tea leaves tend to pile up at the cup's center. Explain how the Ekman boundary layer at the bottom of the cup is responsible for this, and is also responsible for an overall circulation of water inward along the cup's bottom, upward at its center, outward near its top, and downward near its sides. Give a semiquantitative analysis of this phenomenon (the pressures involved, the Eckman-layer thickness, the speeds of flow, etc.)

****

15.5 Sound Waves

So far, our discussion of fluid dynamics has mostly been concerned with flows that are sufficiently slow that the density can be treated as constant. We now introduce the effects of compressibility by discussing sound waves (in a *non*-rotating reference frame). Sound waves are prototypical scalar waves and therefore are simpler in many respects than vector electromagnetic waves and tensor gravitational waves. In the small-amplitude limit, we linearize the Euler and continuity (mass conservation) equations to obtain

$$\rho\frac{\partial \mathbf{v}}{\partial t} = \boldsymbol{\nabla}\delta P\ , \tag{15.66}$$

$$\frac{\partial \delta\rho}{\partial t} = -\rho\boldsymbol{\nabla}\cdot\mathbf{v}\ . \tag{15.67}$$

As the flow is irrotational (vanishing vorticity before the wave arrives implies vanishing vorticity as it is passing), we can introduce a velocity potential so that $\mathbf{v} = \boldsymbol{\nabla}\psi$. Inserting this into Eqs. (15.66) and (15.67) and combining them, we obtain the dispersion-free wave equation

$$\nabla^2\psi = \frac{1}{c^2}\frac{\partial^2\psi}{\partial t^2}\ , \tag{15.68}$$

where

$$c = \left[\left(\frac{\partial P}{\partial \rho}\right)_s\right]^{1/2} \tag{15.69}$$

is the adiabatic sound speed. Note that the derivative must be performed at constant entropy s because there will generally not be time in a single period for heat to cross a wavelength. For a perfect gas, $c = (\gamma P/\rho)^{1/2}$ where γ is the ratio of specific heats. The sound speed in air at 20°C is 340m s^{-1}. In water under atmospheric conditions, it is about 1.5km s^{-1} (not much different from sound speeds in solids).

The general solution of the wave equation (15.68) for plane sound waves propagating in the $\pm x$ directions is

$$\psi = f_1(x - ct) + f_2(x + ct) , \tag{15.70}$$

where f_1, f_2 are arbitrary functions.

We shall use sound waves to illustrate how waves carry energy. The energy density, given in Table 12.1 with $\Phi = 0$, is a sum of two terms, a kinetic energy density $\rho v^2/2$ plus an internal energy density which can be computed by Taylor expansion. If u is the internal energy per unit mass, then the internal energy per unit volume is given by

$$u\rho = [u\rho] + \left[\left(\frac{\partial(u\rho)}{\partial\rho}\right)_s\right]\delta\rho + \frac{1}{2}\left[\left(\frac{\partial^2(u\rho)}{\partial\rho^2}\right)_s\right]\delta\rho^2 \tag{15.71}$$

where the three coefficients in brackets [] are evaluated at the equilibrium density. The first term in Eq. (15.71) just describes the energy of the background fluid. The second term will average to zero over a cycle of the wave. The third term can be simplified using the first law of thermodynamics in the form $du = Tds - Pd(1/\rho)$, followed by the definition $h = u + P/\rho$ of enthalpy density, followed by the first law in the form $dh = Tds + dP/\rho$, followed by expression (15.69) for the speed of sound. We find that

$$\left(\frac{\partial^2(u\rho)}{\partial\rho^2}\right)_s = \left(\frac{\partial h}{\partial\rho}\right)_s = \frac{c^2}{\rho} , \tag{15.72}$$

Hence, the total energy per unit volume carried by the wave, averaged over a wavelength, is

$$\varepsilon = \frac{1}{2}\rho\overline{v^2} + 12c^2\rho\overline{\delta\rho^2} = \frac{1}{2}\rho\left[\overline{(\nabla\psi)^2 + \frac{1}{c^2}\left(\frac{\partial\psi}{\partial t}\right)^2}\right] = \rho\overline{\boldsymbol{\nabla}\psi^2} , \tag{15.73}$$

where we have used $\delta\rho/\rho = v/c = \boldsymbol{\nabla}\psi/c$ from the linearized equation of continuity, (15.67). Thus, there is equipartition of energy between the kinetic and internal energy terms.

The energy flux, given in Table 12.1 with $\Phi = 0$, is the sum of a kinetic energy flux and an internal energy flux. However, the kinetic term is third order in the velocity perturbation and therefore vanishes on average. If we expand the enthalpy as

$$h = h_o + \left(\frac{\partial h}{\partial p}\right)_{s0} = h_o + \frac{\delta p}{\rho} \tag{15.74}$$

then we can write the energy flux as

$$F = \overline{\rho v h} = \overline{\delta p v} = \rho\overline{\boldsymbol{\nabla}\psi\left(\frac{\partial\psi}{\partial t}\right)} = \varepsilon c . \tag{15.75}$$

The energy flux is therefore the product of the energy density and the wave speed, as we might have anticipated.

In Sec. 6.3 we used the above equations for the sound-wave energy density ϵ and flux F to illustrate, via geometric-optics considerations, the behavior of wave energy in a time-varying medium.

Sound waves are nondispersive and so there is no distinction between group velocity and phase velocity. When studying waves in plasmas (Chaps. 20 and 22) we shall return to the issue of energy transport, and shall see that just as information in waves is carried at the group velocity, not the phase velocity, energy is also carried at the group velocity.

The energy flux carried by sound is conventionally measured in dB (decibels). This is defined by the formula

$$dB = 120 + 10\log_{10}(F) \tag{15.76}$$

where the energy flux F is measured in W m^{-2}. Normal conversation is about 50-60dB. Jet aircraft and rock concerts can cause exposure to more than 120dB with consequent damage to the ear.

15.5.1 Sound Generation

So far, we have been concerned with describing how different types of waves propagate. It is also important to understand how they are emitted. We now outline some aspects of the theory of sound generation. The reader should be familiar with the theory of electromagnetic wave emission. There, it is supposed that there is a localised region containing moving charges and consequently variable currents. The source can be described as a sum over electric and magnetic multipoles, and each multipole in the source produces a characteristic angular variation of the distant radiation field. The radiation-field amplitude decays inversely with distance from the source and so the Poynting flux varies with the inverse square of the distance. Integrating over a large sphere gives the total power radiated by the source, broken down into the power radiated by each multipolar component. The most powerful radiating multipole is the electric dipole and the average power associated with it is given by the Larmor formula

$$P = \frac{\overline{\ddot{\mathbf{d}}^2}}{6\pi\epsilon_0 c^3}\ , \tag{15.77}$$

where $\ddot{\mathbf{d}}$ is the second time derivative of the electric dipole moment in the source and the bar denotes a time average.

This same procedure can be followed when describing sound generation. However, as we are dealing with a scalar wave, sound can have a monopolar source. Let us set a small solid sphere, surrounded by fluid, into radial oscillation and compute the far-field fluid oscillations that it produces. Let the surface of the sphere have radius $a + \delta a \exp(-i\omega t)$, where $c/\omega \gg a \gg \delta a$. As the waves will be spherical, the relevant solution of the wave equation (15.68) is

$$\psi = \frac{f(r - ct)}{r}\ , \tag{15.78}$$

where f is a function to be determined. We presume that the sphere is deep inside its near zone, i.e., that the wavelength of the emitted sound waves is large compared to the sphere's radius. Then the fluid's velocity perturbation at the sphere's surface is $\nabla\psi \simeq -f/r^2\mathbf{e}_r$, and we must equate this to the velocity of the surface itself. The result is

$$\psi(r,t) = \frac{i\omega a^2[\delta a]_{ret}}{r} , \tag{15.79}$$

where $[]_{ret}$ signifies evaluation at the retarded time, $t - r/c$. It is customary to express the radial velocity perturbation v in terms of $q = 4\pi\rho a^2\partial\psi/v$, the total radial discharge of air mass crossing an imaginary fixed spherical surface of radius slightly larger than that of the oscillating sphere: $v = \partial\psi/\partial r = q/4\pi\rho a^2$. Using this notation and Eq. (15.79), we compute for the power radiated [Eq. (15.75) integrated over a sphere]

$$P = \frac{\overline{\dot{q}^2}}{4\pi\rho c} \tag{15.80}$$

Note that the power is inversely proportional to the signal speed. This is characteristic of monopolar emission and in contrast to the inverse cube variation for dipolar emission [Eq. (15.77)].

The emission of monopolar waves requires that the volume of the emitting solid body oscillate. When the solid simply oscillates without changing its volume, for example the reed on a musical instrument, dipolar emission should generally dominate. We can think of this as two monopoles in antiphase separated by some displacement δd. The velocity potential in the far field is then the sum of two monopolar contributions, which almost cancel. Making a Taylor expansion, we obtain $\psi_{dipole} \sim \psi_{monopole}(\omega\delta d/c)$.

This reduction of ψ by a factor $\omega\delta d/c$ implies that the dipolar power emission is weaker than monopolar power by a factor $\sim (\omega\delta d/c)^2$ for similar freqencies and amplitides of motion. However, to emit dipole radiation, momentum must be given to and removed from the fluid. In other words the fluid must be be forced by a solid body. In the absence of such a solid body, the lowest multipole that can be radiated effectively is quadrupolar radiation, which is weaker by yet one more factor of $(\omega\delta d/c)^2$.

These considerations are important to understanding how noise is produced by the intense turbulence created by jet engines, especially close to airports. We expect that the sound emitted by the free turbulent flow will be quadrupolar. If we consider turbulent eddies of size $\sim l$ and speed $\sim v_l$, the characteristic frequency radiated will be $\omega \sim v_l/l$. The quadrupolar power radiated per unit volume in the frequency interval from ω to 2ω is, from the above considerations,

$$P \sim \frac{\rho v_l^3}{l}\left(\frac{v_l}{c}\right)^5 \tag{15.81}$$

This is almost certainly dominated by the largest eddies present. For air of fixed sound speed and length scale, and for which the largest eddy speed is proportional to some characteristic velocity V, the sound generation increases proportional to the eighth power of the Mach number $M = V/c$ with obvious implications for the design of jet engines. This is known as Lighthill's law.

****

EXERCISES

Exercise 15.9 *Problem: Aerodynamic Sound Generation*
Consider the emission of quadrupolar sound by a Kolmogorov spectrum of free turbulence. Show that the power radiated per unit frequency interval has a spectrum

$$P_\omega \propto \omega^{-7/2}$$

Also show that the total power radiated is roughly a fraction M^5 of the power dissipated in the turbulence, where M is the Mach number.

****

Bibliography

Gill, A. E. 1982. *Atmosphere Ocean Dynamics*, New York: Academic Press.

Greenspan, H. P. 1973. *The Theory of Rotating Fluids*, Cambridge: Cambridge University Press.

Libbrecht, K. G. & Woodard, M. F. 1991. *Science*, **253**, 152.

Lighthill, M. J. 1978. *Waves in Fluids*, Cambridge: Cambridge University Press.

Whitham, G. B. 1974. *Linear and Non-Linear Waves*, New York: Wiley.